Optical Wire Guided Lumpectomy

A. L. Dayton[a], V.T. Keränen[b] and S. A. Prahl[a]
[a] BME Dept., Oregon Health & Science University, Portland, Oregon, United States
[b] Measurement and Sensor Laboratory, University of Oulu, Kajaani, Finland

ABSTRACT

In practice, complete removal of the tumor during a lumpectomy is difficult to accomplish. Published rates of positive margins, range from 10% to 50%. A spherical lumpectomy specimen with tumor directly in the middle must be obtained more frequently. The proposed optical technique may provide a practical means by which all surgeons may achieve such a resection. It has been shown that the intensity of light sources can be sinusoidally modulated and will predictably become demodulated upon propagation through a scattering medium.

In this work, the modulated light within the medium was collected by optical fiber(s) fixed distance(s) from the source and used to measure the optical properties of the area. The optical properties were then used to calculate the distance the light had traveled through the medium. The fiber was coupled to an 830 nm diode laser that was modulated at 100, 200 and 300 MHz. A handheld optical probe collected the modulated light and a network analyzer measured the phase lag. This data was used to calculate the distance the light traveled from the emitting fiber tip to the probe. An optical phantom as well as a prophylactic mastectomy specimen were used to explore the feasibility of the system.

The optical properties were $\mu_a = 0.004\,\mathrm{mm}^{-1}$ and $\mu_s' = 0.38\,\mathrm{mm}^{-1}$ in the phantom. The optical properties for the tissue were $\mu_a = 0.005\,\mathrm{mm}^{-1}$ and $\mu_s' = 0.20\,\mathrm{mm}^{-1}$. The prediction of distance from the source was within 4 mm of the actual distance at 30 mm in the phantom and within 3 mm of the actual distance at 25 mm in the tissue. The feasibility of a frequency domain system that makes measurements of local optical properties then extrapolates those optical properties to make measurements of distance with a separate probe was demonstrated.

keywords: breast cancer, frequency domain, pathlength, distance, *ex vivo* optical properties, lumpectomy

1. INTRODUCTION

1.1 Lumpectomy for non-palpable tumors is not accurate enough

For small breast cancers and pre-cancerous conditions a lumpectomy, also called breast conserving surgery, is often performed. In this surgical technique, the lesion and surrounding tissue are removed but the remainder of the breast is left intact. Many studies have shown that obtaining negative margins at initial lumpectomy decreases the risk of ipsilateral recurrence and the need for additional surgeries. However, the rate of published negative margins ranges from 50–90% [1–7] and should be improved.

1.2 Significance

In the U.S., 200,000 women were diagnosed with breast cancer and another 50,000 were diagnosed with breast cancer *in situ* in 2005; 40,000 women died of the disease.[8] In 2006, 18,000 inpatient lumpectomies occurred[9] and in 1996, the last year the National Survey of Ambulatory Surgery was completed, 341,000 outpatient lumpectomies were performed. The occurrence of breast conserving surgery has increased in the last decade[10–14] so the actual number of procedures performed in 2009 is likely to be higher. It has been demonstrated that lumpectomies followed by breast irradiation have equivalent 12 year ipsilateral recurrence rate as mastectomies for tumors less than 40 mm in diameter with negative or positive axillary lymph nodes.[15,16] However, the margin status of lumpectomies is critical to the success of the treatment. If a margin is positive following lumpectomy, the patient usually undergoes a second surgery to clear the margins. This not only creates additional cost but also prolongs the course of treatment.

Send correspondence to prahl@bme.ogi.edu, OMLC, PSVMC, 9205 SW Barnes Rd., Portland, OR 97225

1.3 Standard Wire Guided Lumpectomy

More than 25 years ago Daniel Kopans introduced the hookwire technique to simplify the preoperative localization of breast cancers.[17] The hookwire is a 250 mm long thin wire bent at the tip to form a V shaped hook and is now referred to as the Kopans Wire. In practice, a radiologist places a needle in a tumor using either x-ray or ultrasound guidance then slides the Kopans wire, hook end first, through the needle. Once the hook has moved past the end of the needle it springs open in the middle of the tumor and anchors its position. The needle is removed and the wire external to the skin is taped in place to prevent displacement of the wire. Proper placement is confirmed with orthogonal mammograms and the patient is sent to the operating room.

The surgery is guided by the Kopans wire. The surgeon views the mammograms and observes the general location of the tumor and wire. During the operation the wire is followed. Before reaching the end of the wire, the surgeon must deviate from the wire and then re-approach it to excise the tissue surrounding its tip. However, the exact point to deviate from and approach the wire is unclear.

1.4 Optical Wire Guided Lumpectomy

It was hypothesized that illuminating the tissue surrounding tumors would result in more successful lumpectomies. Eight patients have been enrolled in a feasibility phase I clinical trial in which the surgery was guided by a light source, a glowball, imbedded in the tumor. The glowball has facilitated a direct surgical approach to the tumor as well as provided a spherically shaped visible guide for resection.

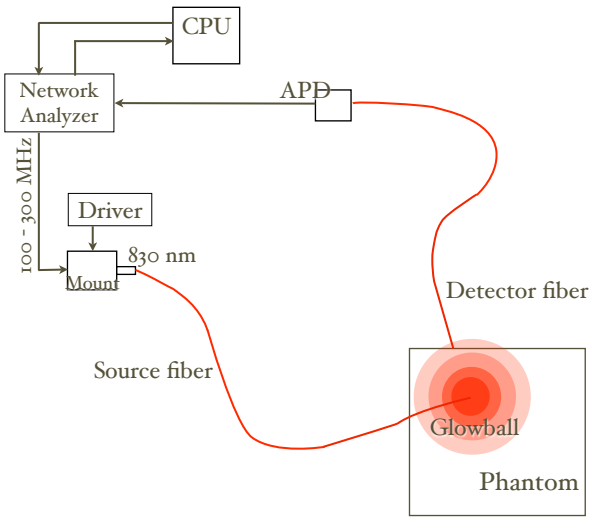

Figure 1. Frequency modulation system.

However, it has become clear that light coupling, ambient lighting, eye sensitivity, and the optical properties of breast tissue affect the perceived size of the glowball, and consequently the actual size of the resection. This variability in perceived size can be negated with quantitative measurements of the light exiting the tissue. Adding an intensity modulated light source to the tip of the Kopans wire could allow for intra-operative measurements of the distance from the source to the surgical cutting plane. Using this procedure, optical wire lumpectomies could result in a decrease in positive margins and in more uniform margins. This could result in fewer procedures, reduced cost, and better cosmesis. A system to accomplish this intera-operative measurements is explored in an optical phantom as well as in *ex vivo* breast tissue.

2. MATERIALS & METHODS

2.1 Frequency Domain system

To test the feasibility of an experimental measurement to calculate the distance, r, based on phase measurements, a system was constructed Figure 1. A network analyzer (Hewlett Packard, 8752C) generated a radio frequency (RF) signal of 100, 200, & 300 MHz. The RF signal was delivered to a laser diode mount (ThorLabs,TCLDM9) on which an 830 nm fiber pigtailed laser diode (Sanyo, DL7032-001) was mounted. The laser diode was also driven by a direct current from the driver (ThorLabs, LDC 210). The sinusoidally modulated light was delivered to a phantom through a 200 μm diameter optical fiber and detected with another 1000 μm diameter optical fiber. The detected signal was coupled to an avalanche photodiode, APD, (ThorLabs, APD 210) where it was converted to voltage and fed back into the network analyzer. Calibration of the system was performed by approximating the source and detector fibers to set a phase lag of 0^o.

To solve for the optical properties of the medium, unconstrained nonlinear optimization was used in Matlab (Mathworks, v 7.4). Using the mean values of the measured phase at specific distances and modulation frequencies by[18,19]

$$\theta(r,\omega) = -r\sqrt{\frac{b}{\alpha}}\left(1+\frac{\omega^2}{b^2}\right)^{1/4}\sin\left(\frac{1}{2}\tan^{-1}\frac{\omega}{b}\right) \quad (1)$$

Where c is the speed of light in medium, $b = \mu_a c$, $\alpha = c/3(\mu_s' + \mu_a)$, $\omega = 2\pi f$, μ_a is the absorption coefficient and μ_s' is the reduced scattering coefficient and equals $\mu_s(1-g)$ where g is the anisotropy and μ_s is the scattering coefficient. Equation 1 was used to find values of the absorption and reduced scattering coefficients for a limited data set. Then, using the phase measurements at all points and the predicted optical properties of the medium, the distance the light had traveled was calculated by:

$$r = -\frac{\theta}{\sqrt{\frac{b}{\alpha}}\left(1+\frac{\omega^2}{b^2}\right)^{1/4}\sin\left(\frac{1}{2}\tan^{-1}\frac{\omega}{b}\right)} \quad (2)$$

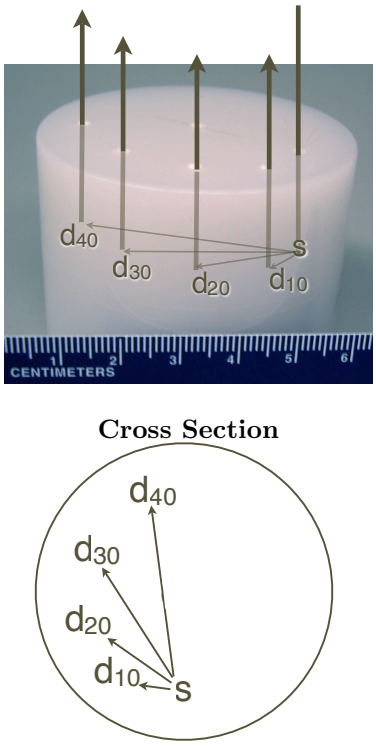

Figure 2. Experimental set up indicating location of source fiber (S) and detector fiber (d_x) positions where x indicates the path length between source and detector in mm. **A.** The polyurethane phantom with fiber locations indicated by thick arrows within the phantom. **B.** Cross section of the phantom in the plane of the fiber tips.

2.2 Polyurethane Phantom

A polyurethane phantom was created. India ink (PRO ART, Beaverton, OR) and titanium dioxide, TiO_2(Sigma, St. Louis MO) were added to polyurethane components (BJB Enterprises, Inc.), which were then mixed and allowed to cure.[20] Polyurethane was made from two components; component A was unreacted polyurethane and component B was catalyst. India ink was mixed with component A and $TiO_2$was mixed with component B. Each component was then placed in a vacuum chamber for degassing, the solutions were held at a reduced pressure until all air bubbles were drawn out of solution. The two components, A:B, were then mixed together in a 100:85 weight ratio respectively. After mixing, the uncured polyurethane was degassed again and then cast into a mold. A cylindrical phantom was cast approximately 60 mm in diameter and 60 mm in height. This served as the tissue simulating phantom. A phantom approximately 60 mm in diameter and 3 mm thick was cast from the same solution; integrating sphere measurements were made on this phantom.

Holes were drilled axially through the cylindrical phantom to half the height of the cylinder as shown in Figure 2A, S indicates the location of the source fiber and d_x indicates the locations of the detector fiber where x is the path length between source and detector in mm. Figure 2B is a cross section of the plane at the tip of the fibers. Phase measurements were made within the holes of the phantom at four locations, 10, 20, 30 & 40 mm from the source. The phase was recorded for each distance (i.e. 10 mm was measured then 20 mm, then 30 mm, then 40 mm) and was repeated 4 times Figure 3 *left*.

The data set used to solve for the optical properties of the phantom held the source-detector separation fixed at $r = 20$ mm. Measurements of the phase, θ, were made at 100, 200 and 300 MHz. Equation 1 was solved with an index of refraction of $n = 1.468$.

2.2.1 Phantom Characterization

To determine the optical properties of the cured polyurethane, integrating sphere measurements were made of the 3 mm thick phantom. A Xenon light was coupled to a 1 mm diameter fiber and used to make both reflectance and transmittance measurements with an integrating sphere (203.2 mm diameter sphere, 44.5 mm diameter sample

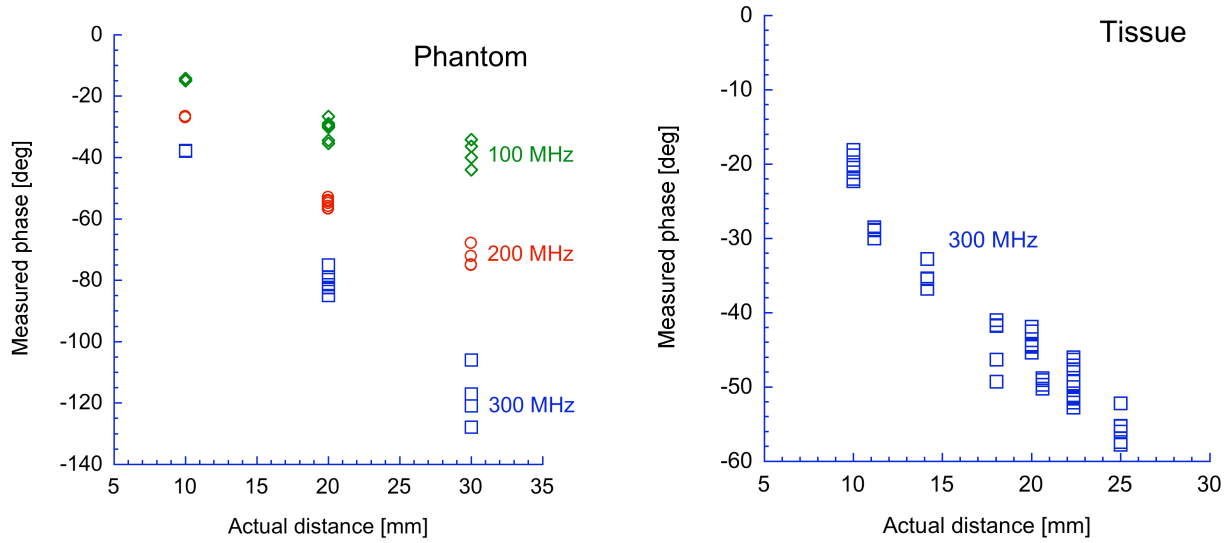

Figure 3. The measured phase as a function of source detector separation distance in the phantom and breast tissue. Squares indicate a modulation frequency of 300 MHz, circles 200 MHz, and diamonds 100 MHz.

port, 6.4 mm entrance port, 0.05 mm diameter illumination beam). The integrating sphere used a 1 mm diameter fiber to couple light into a spectrometer (ISA Horiba) and then a PMT (Products for Research, Inc.) to measure M. Dark noise, M_{dark}, and 100%, M_{100}, signals were measured for reflectance and transmission. A certified reflectance standard (Labsphere) was used for the 100% reflectance measurements. The signal, M was normalized as follows corresponding to either reflectance, R, or transmission, T.

$$R = \frac{M - M_{dark}}{M_{100} - M_{dark}} \qquad T = \frac{M^{'} - M^{'}_{dark}}{M^{'}_{100} - M^{'}_{dark}} \tag{3}$$

Three reflectance and three transmission measurements were taken. An inverse adding-doubling method was used to calculate the absorption coefficient, μ_a, and the reduced scattering coefficient $\mu_{s'}$ from the normalized R and T measurements.

2.3 Tissue Specimen

Following IRB approved protocol, one patient undergoing prophylactic bilateral mastectomy was informed and consented. A cancer-free breast tissue specimen was brought to the lab before pathologic analysis. The specimen had very little skin, approximately 10 % of the surface, and was primarily fatty tissue. A needle was inserted diagonally through the tissue from the top to the side far from skin. A 1 mm optical fiber was inserted through the needle and the needle was removed from the tissue. The tip of the optical fiber was in the plane of the side of the tissue and then retracted to a depth of 10 mm. The detector fiber was placed on the surface at 0, 5, 10, 15 and 20 mm from the point of insertion (white dots in Figure 4). The source fiber was then retracted another 10 mm and the measurements repeated. Source detector separation distance was calculated based on the assumption that a 90^o angle between the source fiber and the tissue surface existed. Data was collected at 300MHz and a refractive index of 1.38 was used in calculations. Two distances, 10 and 14 mm were used to solve for optical properties using Equation 1. Equation 2 was used to calculate the predicted distance for all other source-detector combinations.

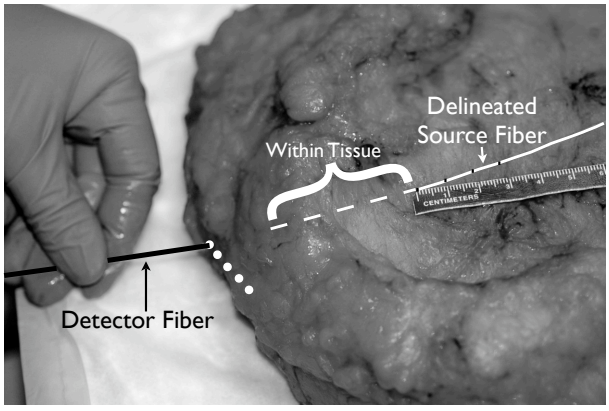

Figure 4. Source and detector positions within the breast tissue.

3. RESULTS & DISCUSSION

3.1 Optical Properties

The absorption and reduced scattering coefficients of the polyurethane phantom are given in Figure 5. The optical properties found from integrating sphere measurements were $\mu_a = 0.003 \pm 0.001(\text{SD})\,\text{mm}^{-1}$ $\mu_s' = 0.41 \pm 0.06(\text{SD})\,\text{mm}^{-1}$ at $\lambda = 830\,\text{nm}$. The predicted optical properties from frequency domain measurements were $\mu_a = 0.004\,\text{mm}^{-1}$ and $\mu_s' = 0.38\,\text{mm}^{-1}$. Both methods produced optical properties within one standard deviation of each other.

The optical properties predicted for the tissue were $\mu_a = 0.005\,\text{mm}^{-1}$ and $\mu_s' = 0.20\,\text{mm}^{-1}$ which are within the limits of published values for breast tissue.[21–47]

	Integrating Sphere [mm^{-1}]	Standard Deviation [mm^{-1}]	Frequency Domain [mm^{-1}]
μ_a	0.003	0.001	0.004
μ_s'	0.41	0.06	0.38

Figure 5. Optical properties of the polyurethane phantom as measured by integrating sphere and frequency domain techniques.

3.2 Phantom Distance Measurements

Figure 6 *top* gives the measured values of phase at 20 mm for 100, 200, & 300 MHz in the phantom as well as the predicted values based on the optical properties that were found to satisfy Equation 1. The distance the light traveled was calculated for the remaining data at 300 MHz and is shown in Figure 7A, where the predicted distance is plotted against the actual distance. Despite the variation in measured optical properties between the integrating sphere & frequency domain techniques, the prediction of distance from the source was within 4 mm of the actual distance of 30 mm in the phantom. Phase measurements were taken at source-detector separation of 40 mm but the signal was not strong enough for reliable measurements and was therefore excluded from analysis. The residuals (actual r - predicted r) are plotted in Figure 7C and range between ±4 mm.

3.3 Tissue Distance Measurements

Figure 6 *bottom* gives the measured values of phase at 300 MHz for 10 & 14 mm in the tissue as well as the predicted values based on the optical properties that were found to satisfy Equation 1. The distance the light traveled was calculated for the remaining data at 300 MHz and is shown in Figure 7B, where the predicted distance is plotted against the actual distance. The residuals (actual r - predicted r) are plotted in Figure 7D and also range between ±4 mm.

As expected, the residuals increased with distance from the source within the phantom, however the same effect was not seen in the tissue. This could be a result of the changing sampling volume within the tissue, and may have also been confounded by changes in the pressure applied by the detector fiber. Ideally, the device should be able to measure distances of 40–50 mm in any direction from the source and more work is being done to accomplish this goal. Despite a need for improvements in range, the current 4 mm margin of error should be clinically acceptable. The feasibility of using either a two frequency, as in the phantom, or two distance, as in the

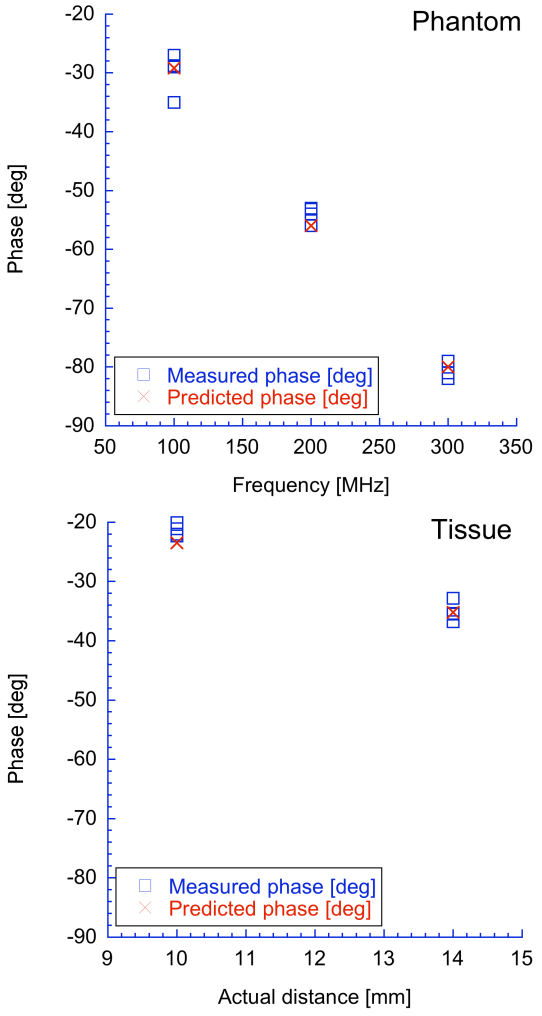

Figure 6. The limited data sets used to solve for the phase in Equation 1. Squares are the measured phase and circles are the predicted values based on the solution to Equation 1

tissue, system to make measurements of local optical properties then extrapolating those optical properties to make a measurement of distance with a separate probe was demonstrated.

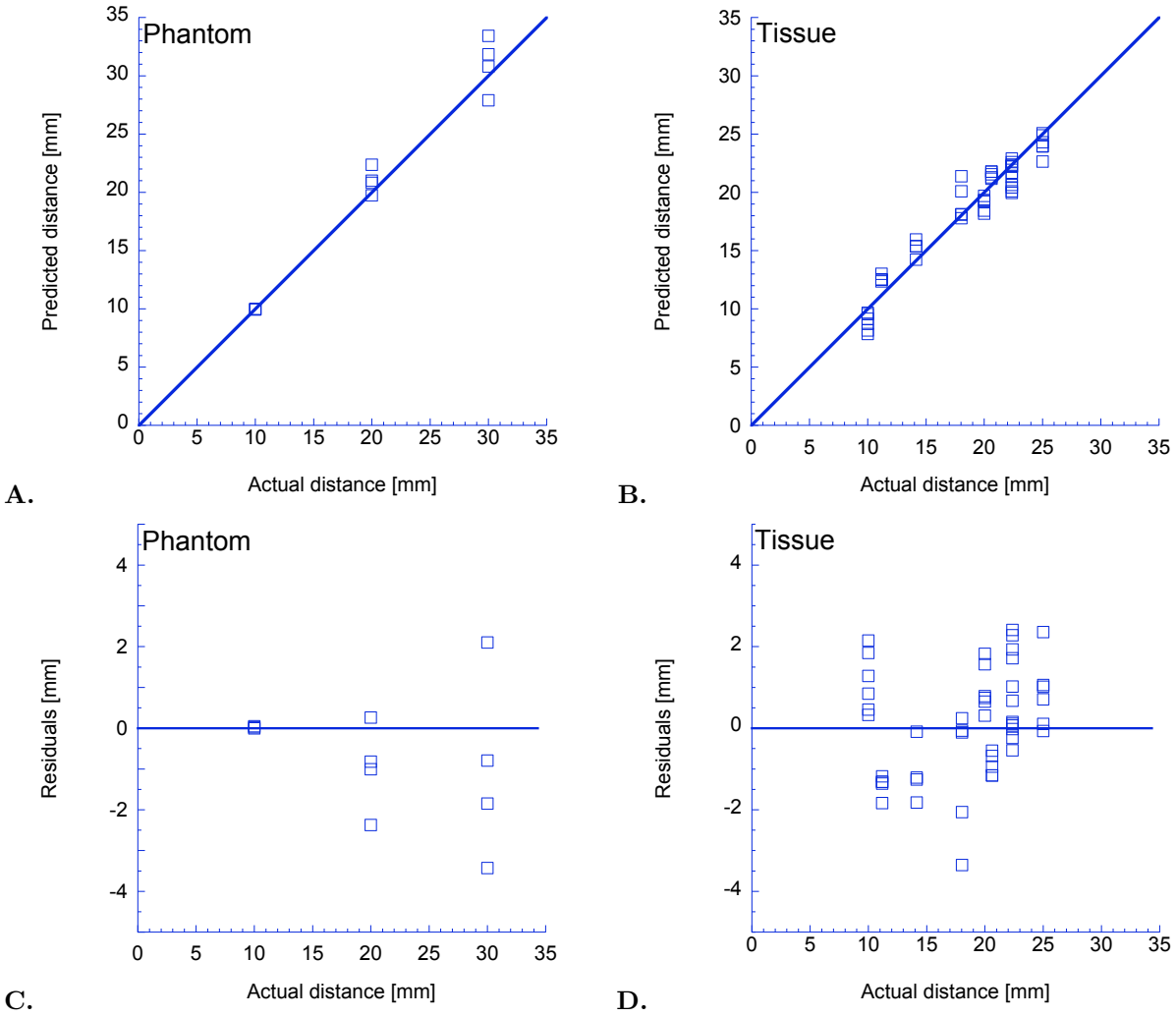

Figure 7. **A.**&**B.** show the predicted values of distance for each phase measurement. **C.**&**D.** are the residuals of the difference between the actual distance and the predicted distance.

REFERENCES

1. S. Renton, J. Gazet, H. Ford, C. Corbishley, and R. Sutcliffe, "The importance of the resection margin in conservative surgery for breast cancer," *European Journal of Surgical Oncology* **22**, pp. 17–22, Feb 1996.
2. H. Luu, C. Otis, W. Reed, J. Garb, and J. Frank, "The unsatisfactory margin in breast cancer surgery," *American Journal of Surgery* **178**, pp. 362–366, Nov 1999.
3. E. Obedian, MD and B. G. Haffty, MD, "Negative margin status improves local control in conservatively managed breast cancer patients," *The Cancer Journal from Scientific American* **6**, pp. 28–33, Jan-Feb 2000.
4. P. Tartter, J. Kaplan, I. Bleiweiss, C. Gajdos, A. Kong, S. Ahmed, and D. Zapetti, "Lumpectomy margins, reexcision, and local recurrence of breast cancer," *American Journal of Surgery* **179**, pp. 81–85, Feb 2000.
5. S. Singletary, "Surgical margins in patients with early-stage breast cancer treated with breast conservation therapy," *American Journal of Surgery* **184**, pp. 383–393, Nov 2002.
6. C. D. Scopa, P. Aroukatos, A. C. Tsamandas, and C. Aletra, "Evaluation of margin status in lumpectomy specimens and residual breast carcinoma," *Breast J* **12**, pp. 150–3, 2006.
7. C. Kotwall, M. Ranson, A. Stiles, and M. S. Hamann, "Relationship between initial margin status for invasive breast cancer and residual carcinoma after re-excision," *American Surgeon* **73**, pp. 337–343, Apr 2007.
8. L. Ries, D. Melbert, M. Krapcho, D. Stinchcomb, N. Howlader, M. Horner, A. Mariotto, B. Miller, E. Feuer, S. Altekruse, D. Lewis, L. Clegg, M. Eisner, M. Reichman, and B. Edwards, "SEER cancer statistics review, 1975-2005," `http://seer.cancer.gov`, 2007.
9. "HCUP national inpatient survey," `http://hcupnet.ahrq.gov`, 2006.
10. C. Kotwall, D. Covington, P. Churchill, C. Brinker, D. Weintritt, and J. G. Maxwell, "Breast conservation surgery for breast cancer at a regional medical center," *Am J Surg* **176**, pp. 510–4, 1998.
11. L. M. Apantaku, "Breast-conserving surgery for breast cancer," *Am Fam Physician* **66**, pp. 2271–8, 2002.
12. B. Jerome-D'Emilia and J. W. Begun, "Diffusion of breast conserving surgery in medical communities," *Soc Sci Med* **60**, pp. 143–51, 2005.
13. F. Fitzal and M. Gnant, "Breast conservation: Evolution of surgical strategies," *Breast Journal* **12**, pp. S165–S173, Sep-Oct 2006.
14. A. Luini, G. Gatti, S. Zurrida, N. Talakhadze, F. Brenelli, D. Gilardi, G. Paganelli, R. Orecchia, E. Cassano, G. Viale, C. Sangalli, B. Ballardini, G. R. dos Santos, and U. Veronesi, "The evolution of the conservative approach to breast cancer," *Breast* **16**, pp. 120–129, Apr 2007.
15. B. Fisher, C. Redmond, E. R. Fisher, M. Bauer, N. Wolmark, D. L. Wickerham, M. Deutsch, E. Montague, R. Margolese, and R. Foster, "Ten-year results of a randomized clinical trial comparing radical mastectomy and total mastectomy with or without radiation," *N Engl J Med* **312**, pp. 674–81, 1985.
16. B. Fisher, S. Anderson, C. K. Redmond, N. Wolmark, D. L. Wickerham, and W. M. Cronin, "Reanalysis and results after 12 years of follow-up in a randomized clinical trial comparing total mastectomy with lumpectomy with or without irradiation in the treatment of breast cancer," *N Engl J Med* **333**, pp. 1456–61, 1995.
17. D. B. Kopans, MD and S. DeLuca, MD, "A modified needle-hookwire technique to simplify preoperative localization of occult breast lesions," *Radiology* **134**, p. 781, March 1980.
18. M. Patterson, B. Chance, and B. Wilson, "Time resolved reflectance and transmittance for the noninvasive measurement of tissue optical-properties," *Applied Optics* **28**, pp. 2331–2336, Jun 15 1989.
19. M. Patterson, "Frequency-domain measurements of light propagation," in *Optical-Thermal Response of Laser-Irradiated Tissue*, A. Welch and M. vanGemert, eds., Plenum Press, New York, 1995.
20. T. Moffitt, Y. Chen, and S. Prahl, "Preparation and characterization of polyurethane optical phantoms," *Journal of Biomedical Optics* **11**, p. 041103, July/August 2006.
21. V. G. Peters, D. R. Wyman, M. S. Patterson, and G. L. Frank, "Optical properties of normal and diseased human breast tissues in the visible and near infrared," *Phys Med Biol* **35**, pp. 1317–34, 1990.
22. W. Cheong, S. Prahl, and A. Welch, "A review of the optical-properties of biological tissues," *IEEE Journal of Quantum Electronics* **26**, pp. 2166–2185, Dec 1990.
23. A. Kienle, L. Lilge, M. Patterson, R. Hibst, R. Steiner, and B. Wilson, "Spatially resolved absolute diffuse reflectance measurements for noninvasive determination of the optical scattering and absorption coefficients of biological tissue," *Applied Optics* **35**, pp. 2304–2314, May 1 1996.

24. K. Suzuki, Y. Yamashita, K. Ohta, M. Kaneko, M. Yoshida, and B. Chance, "Quantitative measurement of optical parameters in normal breasts using time-resolved spectroscopy: In vivo results of 30 japanese women," *Journal of Biomedical Optics* **1**, pp. 330 – 334, July 1996.
25. V. Tuchin, "Light scattering study of tissues," *Phys-Usp* **40**, pp. 495–515, May 1997.
26. B. Tromberg, O. Coquoz, J. Fishkin, T. Pham, E. Anderson, J. Butler, M. Cahn, J. Gross, V. Venugopalan, and D. Pham, "Non-invasive measurements of breast tissue optical properties using frequency-domain photon migration," *Philosophical Transactions of the Royal Society of London Series B-Biological Sciences* **352**, pp. 661–668, Jun 29 1997.
27. G. Zacharakis, A. Zolindaki, V. Sakkalis, G. Filippidis, T. G. Papazoglou, D. D. Tsiftsis, and E. Koumantakis, "In vitro optical characterization and discrimination of female breast tissue during near infrared femtosecond laser pulses propagation," *J Biomed Opt* **6**, pp. 446–9, 2001.
28. N. Shah, A. Cerussi, C. Eker, J. Espinoza, J. Butler, J. Fishkin, R. Hornung, and B. Tromberg, "Noninvasive functional optical spectroscopy of human breast tissue," *Proceedings of the National Academy of Sciences of the United States of America* **98**, pp. 4420–4425, Apr 10 2001.
29. V. Chernomordik, D. Hattery, D. Grosenick, H. Wabnitz, H. Rinneberg, K. Moesta, P. Schlag, and A. Gandjbakhche, "Quantification of optical properties of a breast tumor using random walk theory," *Journal of Biomedical Optics* **7**, pp. 80–87, Jan 2002.
30. M. Nair, N. Ghosh, N. Raju, and A. Pradhan, "Determination of optical parameters of human breast tissue from spatially resolved fluorescence: a diffusion theory model," *Applied Optics* **41**, pp. 4024–4035, Jul 1 2002.
31. T. Durduran, R. Choe, J. Culver, L. Zubkov, M. Holboke, J. Giammarco, B. Chance, and A. Yodh, "Bulk optical properties of healthy female breast tissue," *Physics in Medicine and Biology* **47**, pp. 2847–2861, Aug 21 2002.
32. A. Pifferi, J. Swartling, E. Chikoidze, A. Torricelli, P. Taroni, A. Bassi, S. Andersson-Engels, and R. Cubeddu, "Spectroscopic time-resolved diffuse reflectance and transmittance measurements of the female breast at different interfiber distances," *Journal of Biomedical Optics* **9**(6), pp. 1143–1151, 2004.
33. L. Spinelli, A. Torricelli, A. Pifferi, P. Taroni, G. M. Danesini, and R. Cubeddu, "Bulk optical properties and tissue components in the female breast from multiwavelength time-resolved optical mammography," *Journal of Biomedical Optics* **9**(6), pp. 1137–1142, 2004.
34. R. L. P. van Veen, H. J. C. M. Sterenborg, A. W. K. S. Marinelli, and M. Menke-Pluymers, "Intraoperatively assessed optical properties of malignant and healthy breast tissue used to determine the optimum wavelength of contrast for optical mammography," *Journal of Biomedical Optics* **9**(6), pp. 1129–1136, 2004.
35. D. Jakubowski, A. Cerussi, F. Bevilacqua, N. Shah, D. Hsiang, J. Butler, and B. Tromberg, "Monitoring neoadjuvant chemotherapy in breast cancer using quantitative diffuse optical spectroscopy: a case study," *Journal of Biomedical Optics* **9**, pp. 230–238, Jan-Feb 2004.
36. D. Grosenick, H. Wabnitz, K. T. Moesta, J. Mucke, M. Moller, C. Stroszczynski, J. Stossel, B. Wassermann, P. M. Schlag, and H. Rinneberg, "Concentration and oxygen saturation of haemoglobin of 50 breast tumours determined by time-domain optical mammography," *Physics in Medicine and Biology* **49**, pp. 1165–1181, Apr 2004.
37. N. Shah, A. Cerussi, D. Jakubowski, D. Hsiang, J. Butler, and B. Tromberg, "Spatial variations in optical and, physiological properties of healthy breast tissue," *Journal of Biomedical Optics* **9**, pp. 534–540, May-Jun 2004.
38. M. Simick, R. Jong, B. Wilson, and L. Lilge, "Non-ionizing near-infrared radiation transillumination spectroscopy for breast tissue density and assessment of breast cancer risk," *Journal of Biomedical Optics* **9**, pp. 794–803, Jul - Aug 2004.
39. D. Grosenick, H. Wabnitz, K. T. Moesta, J. Mucke, P. M. Schlag, and H. Rinneberg, "Time-domain scanning optical mammography: II. optical properties and tissue parameters of 87 carcinomas," *Phys Med Biol* **50**, pp. 2451–68, 2005.
40. T. Svensson, J. Swartling, P. Taroni, A. Torricelli, P. Lindblom, C. Ingvar, and S. Andersson-Engels, "Characterization of normal breast tissue heterogeneity using time-resolved near-infrared spectroscopy," *Phys Med Biol* **50**, pp. 2559–71, 2005.

41. C. Zhu, G. Palmer, T. Breslin, F. Xu, and N. Ramanujam, "Use of a multiseparation fiber optic probe for the optical diagnosis of breast cancer," *Journal of Biomedical Optics* **10**, Mar - Apr 2005.
42. A. Garofalakis, G. Zacharakis, G. Filippidis, E. Sanidas, D. Tsiftsis, E. Stathopoulos, M. Kafousi, J. Ripoll, and T. Papazoglou, "Optical characterization of thin female breast biopsies based on the reduced scattering coefficient," *Physics in Medicine and Biology* **50**, pp. 2583–2596, Jun 7 2005.
43. L. Spinelli, A. Torricelli, A. Pifferi, P. Taroni, G. Danesini, and R. Cubeddu, "Characterization of female breast lesions from multi-wavelength time-resolved optical mammography," *Physics in Medicine and Biology* **50**, pp. 2489–2502, Jun 2005.
44. R. L. P. van Veen, A. Amelink, M. Menke-Pluymers, C. van der Pol, and H. J. C. M. Sterenborg, "Optical biopsy of breast tissue using differential path-length spectroscopy," *Physics in Medicine and Biology* **50**, pp. 2573–2581, Jun 2005.
45. N. Shah, J. Gibbs, D. Wolverton, A. Cerussi, N. Hylton, and B. Tromberg, "Combined diffuse optical spectroscopy and contrast-enhanced magnetic resonance imaging for monitoring breast cancer neoadjuvant chemotherapy: a case study," *Journal of Biomedical Optics* **10**, Sep - Oct 2005.
46. A. Cerussi, N. Shah, D. Hsiang, A. Durkin, J. Butler, and B. J. Tromberg, "In vivo absorption, scattering, and physiologic properties of 58 malignant breast tumors determined by broadband diffuse optical spectroscopy," *Journal of Biomedical Optics* **11**, Jul - Aug 2006.
47. S. A. Carp, T. Kauffman, Q. Fang, E. Rafferty, R. Moore, D. Kopans, and D. Boas, "Compression-induced changes in the physiological state of the breast as observed through frequency domain photon migration measurements," *Journal of Biomedical Optics* **11**, Nov - Dec 2006.